Femtosecond dynamics of the laser-induced solid-to-liquid phase transition in aluminum

M. Kandyla, T. Shih, and E. Mazur
Department of Physics and Division of Engineering and Applied Sciences, Harvard University, 9 Oxford Street, Cambridge, Massachusetts 02138, USA

(Received 11 December 2006; revised manuscript received 8 April 2007; published 13 June 2007; corrected 21 June 2007)

We present femtosecond time-resolved measurements of the reflectivity of aluminum during the laser-induced solid-to-liquid phase transition over the 1.7–3.5 eV spectral range. Previous optical and electron-diffraction studies have shown discrepancies on the order of picoseconds in the time scale of the solid-to-liquid phase change. As a result, it is not clear if the transition mechanism is thermal or nonthermal. Our experiments conclusively show that this transition is a thermal process mediated through the transfer of heat from the photoexcited electronic population to the lattice. Our findings agree with the results of the electron-diffraction study and rule out the nonthermal mechanism proposed by the optical study.

DOI: 10.1103/PhysRevB.75.214107 PACS number(s): 78.47.+p, 78.40.Kc, 64.70.Dv

I. INTRODUCTION

The dynamical properties of the electrons and the lattice in solids define many basic properties of these materials, such as their conductivity, superconductivity, magnetism, and linear and nonlinear optical properties. Excitation with intense ultrashort laser pulses is one way to induce nonequilibrium processes and observe the resulting dynamics. Previous studies have shown that large laser-induced changes in carrier occupation in metals and semiconductors can lead to substantial band-structure renormalization and even to structural phase transitions.[1–5] An ultrashort laser pulse can rapidly heat electrons to temperatures on the order of 10^3 K while leaving the lattice near room temperature. This transient two-temperature system tends to reach quasiequilibrium within a few picoseconds via electron-phonon interactions, as well as electron diffusion out of the excited region. In the low-intensity regime, the excited region returns to the ground state with no permanent changes. In the high-intensity regime, on the other hand, structural changes such as melting and ablation take place and the morphology of the material is permanently modified. Melting that results from a rise of the lattice temperature above the material's melting point, called thermal melting, can readily be observed with laser pulses of duration longer than 10 ps. After the development of femtosecond lasers, a different, nonthermal melting mechanism was reported in semiconductors.[1,6–10] This mechanism takes place when the ions rapidly gain kinetic energy after the laser-induced electronic excitation and rearrange themselves in a liquidlike, disordered configuration before the lattice has enough time to reach the melting temperature. Nonthermal melting is usually completed within hundreds of femtoseconds after photoexcitation, as opposed to thermal melting which evolves on a picosecond time scale that is set by the electron-phonon coupling constant.

Aluminum was the first metal for which a nonthermal melting mechanism was reported by Guo *et al.*[3] The optical properties of aluminum both in the solid and in the liquid state have been the subject of intense research over the past decades.[11–16] Guo *et al.* performed optical pump-probe measurements of the dielectric constant of aluminum at 800 nm, with femtosecond time resolution. This wavelength, which corresponds to a photon energy of 1.55 eV, is particularly suitable because the absorption of aluminum is enhanced at 800 nm and light can couple into the material more effectively. The enhanced absorption is due to nearly parallel electronic bands around the Fermi energy that are separated by a gap of 1.55 eV and that give rise to an interband contribution to the dielectric function of the material around 800 nm.[17] Guo *et al.* showed that 500 fs after excitation of a solid aluminum sample by a laser pulse, the dielectric constant at 800 nm reaches the value of the dielectric constant for liquid aluminum. Because this time is shorter than the picosecond time scale for lattice thermalization, the material was reported to undergo a nonthermal, electronically induced phase transition. This conclusion was later disputed by Siwick *et al.*,[18] who sent 500-fs-long electron pulses through an optically excited 20-nm-thick aluminum film and studied the resulting electron-diffraction spectra. In these films, the solid-to-liquid phase transition was found to take 3.5 ps and to be a thermal process. Each of the two aforementioned studies has its limitations. The optical pump-probe experiment was performed with high time resolution, down to 130 fs, but it tracked the dynamics of the dielectric constant at a single wavelength only. The electron-diffraction experiment provided a direct picture of the aluminum lattice during the phase transition but it was performed with limited time resolution, only down to 500 fs.

In this paper, we present an optical pump-probe study of the laser-induced solid-to-liquid phase transition in aluminum. We employ a broadband time-resolved reflectometry technique that enables the measurement of the optical properties of aluminum during the solid-to-liquid phase transition over a wide frequency range, from 1.7 to 3.5 eV, with a time resolution of 65 fs. Our findings show that the laser-induced solid-to-liquid phase transition in aluminum is a thermal process that takes place on the picosecond time scale. The observed optical properties over this broad frequency range do not exhibit a subpicosecond time scale, as previously reported.[3] Our data indicate that the dynamics appear faster for photon energies near 1.55 eV, but for higher photon energies, the time scale of the transition is clearly in the picosecond regime.

II. EXPERIMENT

We performed dual-angle-of-incidence reflectometry measurements in a pump-probe setup[19] to measure the changes in the reflectivity of aluminum during the laser-induced solid-to-liquid phase transition. We use a commercial Ti:sapphire oscillator to seed a homebuilt 1 kHz repetition-rate Ti:sapphire multipass amplifier which produces 40 fs, 0.5 mJ pulses at 800 nm.[20] The pump beam consists of a train of 800 nm *s*-polarized pulses that we focus onto a 110-μm-diameter spot on the sample using a 0.2 m focal-length lens. We use a *p*-polarized white-light (1.7–3.5 eV) probe, which we obtain by focusing part of the femtosecond laser-pulse train into a 3-mm-thick piece of CaF_2. To correct for dispersive stretching of this broadband probe pulse, we measured the chirp separately using a Te sample and time shifted the data according to the measured chirp.[21] Measurements of the spectrum and chirp of the white-light probe indicate that the time resolution of the probe varies from 20 fs near 1.7 eV to 65 fs near 3.5 eV.[22] We use a small fraction of the probe beam as a reference beam in order to normalize the effect of pulse energy fluctuations. In order to ensure probing of a homogeneously excited region, the size of the pump beam spot on the sample surface is about four times larger than the probe spot. The angle between the pump and probe beams is kept as small as possible (approximately 13°) to minimize the loss of temporal resolution that accompanies noncollinear pump-probe configurations.

The sample was translated between successive pump laser pulses so that each pump pulse excited an undamaged area. Each data point is averaged over 20 shots. Two sets of reflectivity measurements were taken with the probe beam at angles of incidence of 68.4° and 58.7°. The detection system is calibrated to obtain absolute reflectivity values. Shot-to-shot fluctuations in the white-light probe intensity limit the sensitivity of our apparatus in measuring minimum changes in reflectivity of about 3%–4%.

The polycrystalline 1-μm-thick aluminum samples were prepared by electron-beam evaporation in high vacuum on clean glass microscope slides. The thickness of the films is much greater than the roughly 10 nm penetration depth of the optical fields and thus the samples can be considered to be optically thick. Reflectivity measurements performed on aluminum and Al_2O_3 at laser intensities and wavelengths similar to the ones used in our study have shown that the presence of a thin Al_2O_3 layer does not significantly affect the aluminum metal data.[23]

III. RESULTS

In order to present our measurements on the laser-induced solid-to-liquid phase transition in aluminum in a meaningful way, we first need to determine the melting threshold fluence F_{th} (that is, the minimum incident laser fluence that induces melting on the material surface). To this end, we irradiated an aluminum sample with single pump pulses of varying intensity and examined the resulting surface morphology with a scanning electron microscope. Using this approach, we find that the minimum incident laser fluence required to induce melting is $F_{th}=2.1$ kJ/m^2, a value that is higher than previously reported.[3,18] Guo *et al.*[3] reported an irreversible damage threshold of 0.34 kJ/m^2 and Siwick *et al.*[18] cited the same damage threshold. This discrepancy can be attributed to the difference in film thickness: our samples are 1 μm thick, whereas the previous study used films with a thickness on the order of 20 nm.[18] For 20-nm-thick films, the thickness of the sample is comparable to the ballistic range of the photoexcited electrons. As a result, the film becomes uniformly heated upon electron thermalization and there are no significant hot-electron diffusion effects.[24] This lack of diffusion in very thin films results in a higher energy density stored in the material, and therefore these films require a lower incident fluence for melting to occur. In contrast, in the 1-μm-thick aluminum samples used in this study, the hot electrons diffuse into the bulk of the material. Consequently, the energy deposited by the laser pump pulse is distributed deeper into the material via electron diffusion, resulting in a lower energy density stored near the surface, and therefore a higher melting threshold. A similar dependence of melting threshold on sample thickness has been observed in other materials.[24]

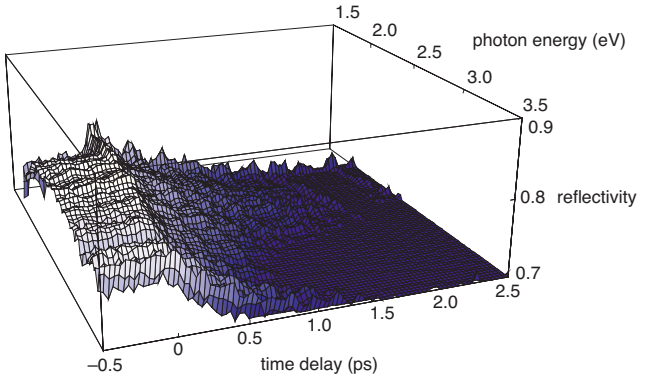

FIG. 1. (Color online) Time-resolved reflectivity dynamics of aluminum following single-pulse photoexcitation across the 1.8–3.5 eV frequency range. The peak absorbed fluence of the incident laser pulse is $3.6F_{th}$.

Figure 1 shows the response of the reflectivity of aluminum across a spectral range of 1.8–3.5 eV following single pulse excitation with a fluence of $3.6F_{th}$. The angle of incidence of the probe is 68.4°. At negative time delays (that is, when the probe arrives before the pump pulse), the reflectivity data agree with ellipsometric measurements of the aluminum sample. At positive time delays (after the arrival of the pump pulse), we observe that the reflectivity starts to drop across all frequencies within our spectral range as the solid-to-liquid phase transition is initiated. The transition is complete after 1.9 ps, as can be seen by the low reflectivity region in Fig. 1. This is when the reflectivity reaches an equilibrium value, which, for all frequencies contained in the white-light probe, is lower than the reflectivity of solid aluminum.

Figures 2(a) and 2(b) show the response of the reflectivity at four different fluences above the melting threshold, with the probe beam incident at 68.4° and 58.7°, respectively. Because 68.4° is closer to the angle for minimum *p* reflec-

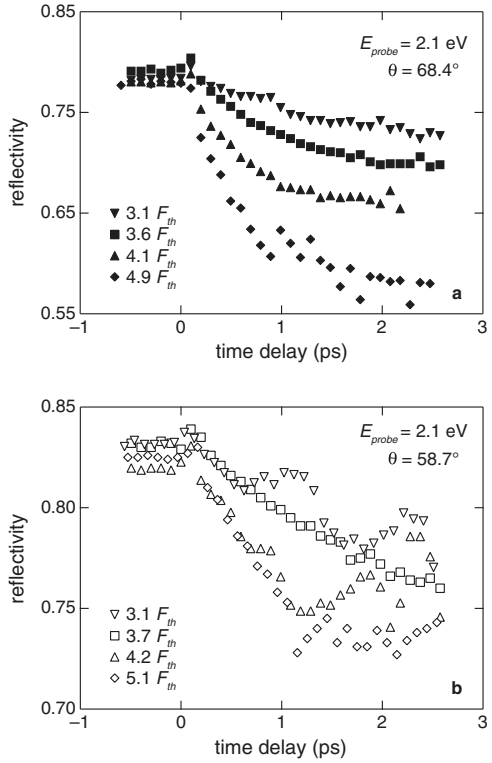

FIG. 2. Time-resolved reflectivity dynamics of aluminum following single-pulse photoexcitation at 2.1 eV for different peak absorbed fluences of the excitation pulse. The reflectivity measurements are taken at probe beam incidence angles of (a) 68.4° and (b) 58.7°.

tivity in aluminum, the sensitivity of the measurements at this angle is higher than the one at 58.7°.[25] The fluences used in Fig. 2 are above the ablation threshold of the aluminum films, as we determined by postirradiation study under an optical microscope. However, because ablation involves transport of large numbers of heavy particles, these processes tend to be slow compared with the time scale of energy thermalization.[26] Ablation therefore occurs outside our time window and we can isolate the solid-to-liquid phase transition that precedes the removal of material from the sample surface.[27,28] The data in Fig. 2 show that for all fluences and angles, the time scale of the laser-induced solid-to-liquid phase transition in aluminum lies in the picosecond regime.

For both angles, the reflectivity in the liquid state decreases as the incident pump fluence increases. Previous measurements have shown that the index of refraction of liquid aluminum increases and the extinction coefficient decreases with increasing temperature.[13,29] Based on these observed changes in index of refraction and extinction coefficient, the Fresnel equations[30] predict a decrease in reflectivity with increasing temperature. The higher fluence data thus suggest that the liquid aluminum reaches a higher temperature, as one would expect.

For sufficiently intense laser pulses, the material can undergo a solid-to-plasma phase transition, without reaching the liquid state. In order to exclude the possibility that the decrease in reflectivity is due to a plasma expansion, we extended the time delay up to 10 ps. Figure 3 shows the

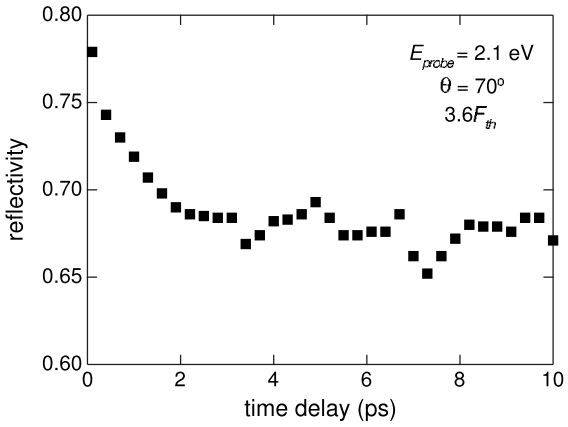

FIG. 3. Time-resolved reflectivity dynamics of aluminum following single-pulse photoexcitation at 2.1 eV. The peak absorbed fluence of the incident laser pulse is $3.6F_{th}$. The reflectivity measurements are taken at an angle of 70°.

time-resolved reflectivity data at 2.1 eV, taken with the probe beam incident at 70°, following excitation by a pump pulse with a fluence of $3.6F_{th}$. Across all frequencies in the white-light probe, we observe a behavior similar to the one shown in Fig. 3: the reflectivity drops for about 2 ps and then remains constant up to 10 ps. In a previous pump-probe experiment,[31] it was shown that the effect of plasma expansion on aluminum results in an initial drop of the reflectivity, followed by a recovery to approximately 60% of the original value within 15 ps. Such a recovery is not present in our findings, indicating that the excitation fluence we used is sufficient to initiate a solid-to-liquid phase transition but not high enough to initiate a detectable plasma expansion process.

IV. DISCUSSION

Our results show that over the entire fluence range studied, the laser-induced solid-to-liquid phase transition in aluminum takes 1.5–2 ps, confirming that the transition is thermal. We extract the picosecond time scale from curves similar to the ones shown in Fig. 2 at all the different frequencies contained in the white-light probe. Because there are 18 such curves at each fluence, it is not possible to show all of them. Instead, we show in Fig. 4 the average of the solid-to-liquid transition time over the frequency range of 2.0–3.3 eV for each fluence. We do not include the edges of our spectral window (1.7–1.9 and 3.4–3.5 eV) in the averaging because the signal-to-noise ratio at these frequencies is significantly smaller compared to the rest of the white-light data points. Figure 4 shows that the average transition time is on the order of picoseconds for all eight fluences and two angles of incidence for which we took measurements. None of the data sets exhibits a femtosecond time scale as reported in Ref. 3. Moreover, the average transition time is nearly independent of fluence, as indicated by the nearly zero slope of the linear least-squares fitted line in Fig. 4. In contrast, for nonthermal phase transitions, the characteristic time of the changing component of the reflectivity gets shorter as the

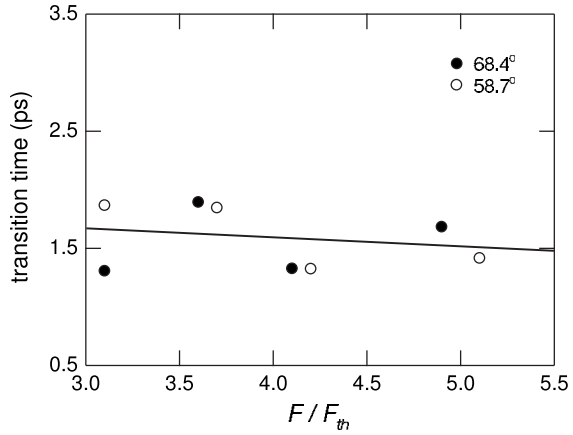

FIG. 4. Average transition times extracted from reflectivity measurements similar to the ones shown in Fig. 2 for different peak absorbed excitation fluences and incidence angles of 68.4° (filled circles) and 58.7° (open circles). Transition times of reflectivity curves in the 2–3.3 eV range were averaged for each fluence. The solid line is the least-squares fit to the data.

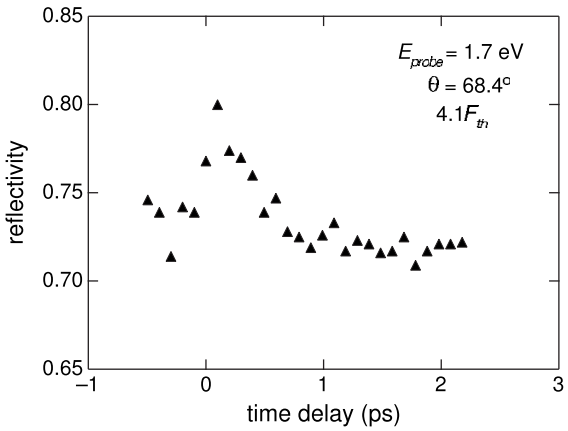

FIG. 5. Time-resolved reflectivity dynamics of aluminum at 1.7 eV following single-pulse photoexcitation. The peak absorbed fluence of the incident laser pulse is $4.1F_{th}$. The reflectivity measurements are taken at a probe incidence angle of 68.4°.

laser fluence increases.[6,7] Therefore, both the picosecond time scale governing the reflectivity dynamics and the independence of this time scale from fluence lead to the conclusion that the laser-induced solid-to-liquid phase transition in aluminum is a thermal process. Furthermore, our time scale is in agreement with calculations based on homogeneous melting of photoexcited materials, which involves the formation of liquid nuclei in the bulk of a superheated crystal.[32] According to the homogeneous model, melting of femtosecond laser-excited aluminum takes a few picoseconds. In contrast, heterogeneous nucleation, where melting starts at the surface and the melt front propagates into the material with a velocity limited by the speed of sound, results in much longer time scales.

Our results agree with those of Siwick *et al.*[18] in that the phase transition is a thermal process, mediated by heat transferred from the excited electronic population to the lattice through electron-phonon coupling. However, the transition times of 1.5–2.0 ps we obtain are shorter than the 3.5 ps obtained in Ref. 18 and the difference cannot be accounted for by the difference in time resolution (65 fs vs 500 fs, respectively). As mentioned in Sec. III, hot-electron diffusion is inhibited for the 20-nm-thick aluminum films of Siwick *et al.* but present for the 1-μm-thick aluminum films used in our study. According to the two-temperature model, diffusion of hot electron results in faster equilibration times between hot electrons and the lattice. Therefore, the lattice temperature exceeds the melting temperature faster in thick photoexcited samples than in thin films,[24] and so the solid-to-liquid transition should occur more quickly in thicker samples, as we observe.

The question remains why the results obtained by Guo *et al.* do not agree with ours, both being obtained from optical measurements with similar time resolution. An important distinction between the two measurements is that while we monitor reflectivity over a broad range of photon energies, Guo *et al.* monitored reflectivity changes only at a single photon energy, the resonance energy in the dielectric function of aluminum. Indeed, our data closest to the aluminum resonant energy of 1.55 eV exhibit faster dynamics than most of the other photon energies contained in the white-light probe (Fig. 5). We observe that the reflectivity at 1.7 eV reaches equilibrium at a time delay of about 800 fs, close to the 500 fs reported by Guo *et al.* and much faster than the reflectivity at 2.1 eV, shown in Fig. 2(a) for the same excitation fluence.

The discrepancy between the results obtained near and away from resonance can be explained by considering the difference in reflectivity of solid and liquid aluminum. Figure 6 shows the reflectivity of solid and liquid aluminum at 68.4°.[11,15] While the difference in reflectivity between solid and liquid is large at most photon energies, it is very small at resonance (1.55 eV) and so measurements obtained at that photon energy are not very sensitive to phase changes. While the experimental method and analysis used in Ref. 3 are

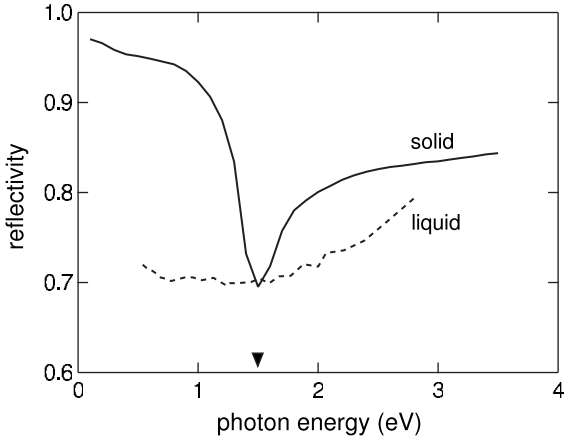

FIG. 6. *p*-polarized reflectivity of solid aluminum (solid line) and liquid aluminum (dashed line) calculated for an incidence angle of 68.4°. Solid aluminum data are from Ref. 11 and liquid aluminum data from Ref. 15. The arrow indicates the position of the interband resonance in solid aluminum at 1.55 eV.

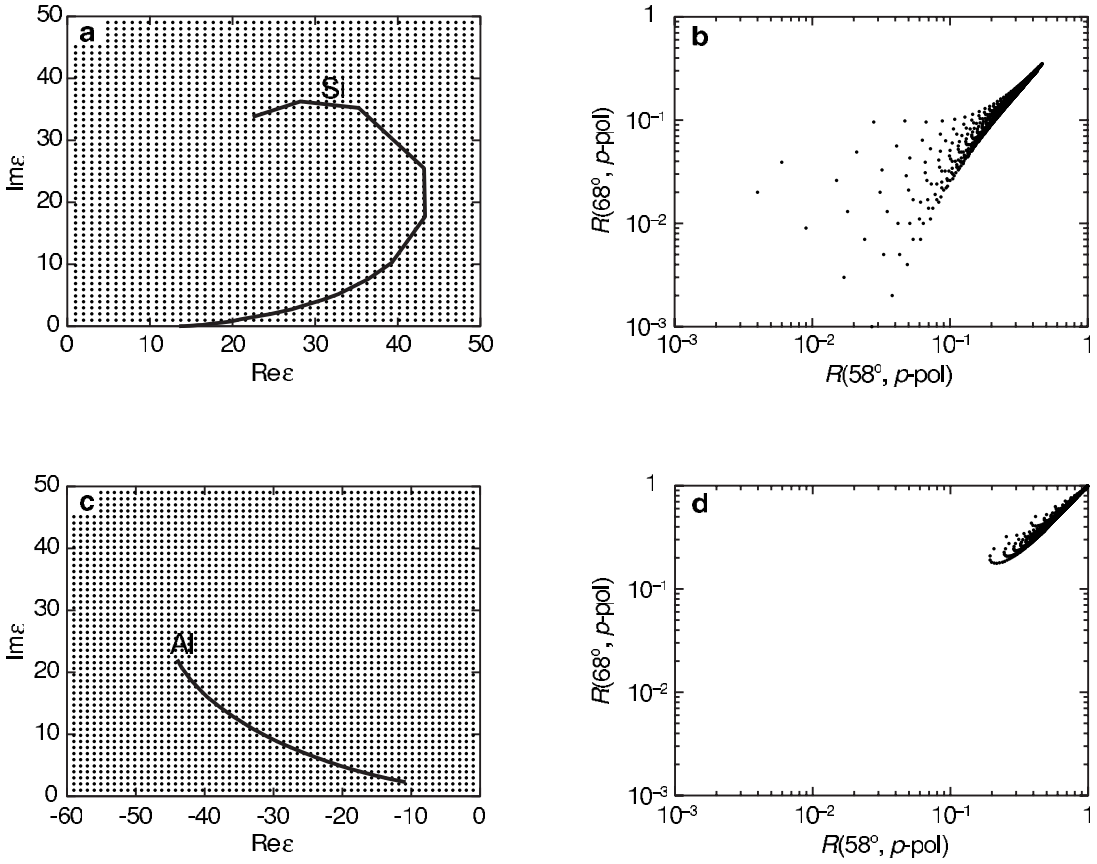

FIG. 7. (a) The dielectric function of silicon (from 1.7 to 3.5 eV) plotted over a grid of dielectric constant values with positive real and imaginary parts. In (b), the Fresnel equations are used to calculate reflectivity pairs at the angles and polarizations indicated for each of the points in (a). (c) The dielectric function of Al (from 1.7 to 3.5 eV) is plotted over a grid of dielectric constant values with negative real parts. In (d), the Fresnel equations are used to calculate reflectivity pairs at the angles and polarizations indicated for each of the points in (c).

valid, the choice of wavelength appears to be unfavorable for studying the time scale of the laser-induced solid-to-liquid phase transition in aluminum.

A more direct way to compare our findings with the results of Guo *et al.*[3] would be to use the Fresnel equations[30] to convert the reflectivity data to dielectric constant data. To determine both the real and the imaginary part of the dielectric constant, one needs two independent reflectivity measurements at two different angles of incidence. Measuring the dielectric constant has fundamental advantages over measuring the reflectivity because the dielectric constant reveals information about the intrinsic optical properties of the material. In the past, dielectric constant dynamics have been successfully determined from reflectivity measurements in semiconducting materials by dual-angle reflectometry.[21,33,34] In Fig. 7, we show the mapping between reflectivity and dielectric constant space by calculating reflectivity pairs over a range of dielectric constant values using the Fresnel equations. Figure 7(a) shows a grid of positive real and imaginary dielectric constant values. For semiconductors such as silicon,[11] the dielectric function has positive real and imaginary parts at most optical frequencies; the dielectric function for silicon from 1.7 to 3.5 eV is superimposed on the grid in Fig. 7(a). Figure 7(b) shows the mapping of this grid onto reflectivity space for *p*-polarized light incident at the angles used in this paper. Figure 7(c) shows a grid of dielectric constant values extended to include negative real dielectric constants, as is often the case for metals such as aluminum.[11] The dielectric function for aluminum from 1.7 to 3.5 eV is superimposed on the grid in Fig. 7(c). Figure 7(d) shows the mapping of this grid onto reflectivity space for the same conditions as in Fig. 7(b). We see that for metals, the result is quite different than for semiconductors: a wide range of dielectric constant values collapses onto a very small range of reflectivity values, and so the experimental uncertainty in the measured reflectivity translates into a large uncertainty in the dielectric constant. For this reason, we report the reflectivity measurements directly rather than convert them to dielectric constant values. For dielectric constant measurements in metals, ellipsometry is more suitable than reflectometry.[11]

In Fig. 2, all the data sets show a sudden increase in reflectivity near $t=0$, followed by a decrease towards the liquid value. This feature is not present in all frequencies contained in the white-light probe, however. It appears at photon energies between 1.7 and 2.5 eV and it is not present at 2.6–3.5 eV. Electron heating results in a drop rather than an increase in reflectivity,[31] and therefore cannot explain the presence of this spike. In single-color pump-probe experiments, the presence of a similar spike near $t=0$ has been attributed to an interference due to the simultaneous arrival

at the sample surface of the pump and probe beams (a "coherent effect").[35–39] Although this coherent effect is more commonly observed in experiments where the pump and probe beams have parallel polarizations, there are various cases where it has been detected with cross-polarized pump and probe beams,[36–39] as is the case in the experiments presented here. In contrast to single-color pump-probe experiments, the pump and probe pulses used in this work have different frequencies, with the pump centered at 1.55 eV and the probe spanning the 1.7–3.5 eV range. Two coherent beams of frequencies ω_1 and ω_2 can cause a coherent effect when $|\omega_2-\omega_1|^{-1}>\tau_{resp}$, where τ_{resp} is the decay time of the impulse response of the material to a delta function excitation.[39] Because each pair of pump and probe pulses is derived from the same laser pulse, the pump and probe beams are coherent. Furthermore, we only observe the effect at the lower end of the frequency range of the probe beam, for which $|\omega_2-\omega_1|^{-1}>\tau_{resp}$, where ω_1 is the frequency of the pump beam. Therefore, we conclude that the spike in the reflectivity near $t=0$ is a coherent effect, often present in pump-probe experiments.

Our data also allow us to extract information about the optical properties of liquid aluminum, which have been a subject of debate.[12–16] Whether liquid aluminum exhibits the same resonance at 1.55 eV as solid aluminum remains an open question. In Fig. 8, we compare reflectivity measurements for the solid and the liquid state of aluminum. The filled circles represent reflectivity spectra taken with the white-light probe at a negative time delay—that is, before the arrival of the pump when the sample is still in the solid state—superimposed on ellipsometric measurements (solid line) of the reflectivity of the same sample at the same angle of incidence. The white-light data agree very well with the ellipsometric data and they confirm the decrease in the reflectivity of solid aluminum around the resonance at 1.55 eV. The open circles in Fig. 8 represent the reflectivity spectrum after the arrival of the pump, when the material has reached the liquid state (1.9 ps). As can be seen, the resonant feature is absent in the liquid state and the reflectivity no longer shows an interband contribution near 1.55 eV. The liquid aluminum reflectivity spectrum shown in Fig. 8 is representative of the entire fluence range we used. Due to the loss of long-range order in the lattice, the parallel band structure is absent in the liquid state of aluminum. It should also be noted that the reflectivity of the laser-induced liquid aluminum state in Fig. 8 differs from the reflectivity of liquid aluminum determined from ellipsometric measurements on molten aluminum (dashed line in Fig. 6). This difference can be attributed to the presence of an excited electronic population in the laser-induced liquid state. Similar differences have been observed in other materials in similar conditions of intense laser excitation.[5]

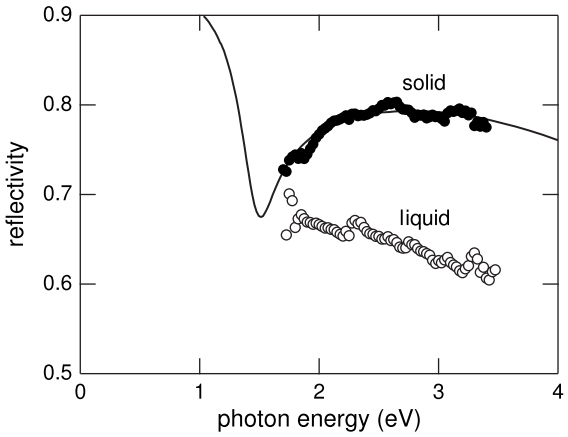

FIG. 8. *p*-polarized reflectivity of solid aluminum, determined by ellipsometry (solid line) and time-resolved reflectometry (filled circles) at 68.4°. *p*-polarized reflectivity of liquid aluminum at 1.9 ps determined by time-resolved reflectometry at the same angle (open circles).

V. CONCLUSION

We present broadband reflectometry data on the laser-induced solid-to-liquid phase transition in aluminum. The time scale of the transition is 1.5–2 ps, indicating that the transition is thermal in nature, in agreement with electron-diffraction studies. The resonance in the optical properties of solid aluminum at 1.55 eV is absent in the liquid state, demonstrating that the parallel band structure is no longer present. The reflectivity of the liquid state is lower than that of the solid state and remains constant over a period of 10 ps, showing no plasma expansion contributions.

ACKNOWLEDGMENTS

We gratefully acknowledge C. Mendonca for valuable discussions and M. Winkler and T. Voss for their role in editing the manuscript. T.S. acknowledges financial support from the NSF Graduate Research Program. The National Science Foundation supported this work under Grant No. DMR-0303642.

[1] P. Saeta, J. K. Wang, Y. Siegal, N. Bloembergen, and E. Mazur, Phys. Rev. Lett. **67**, 1023 (1991).
[2] K. Sokolowski-Tinten, J. Solis, J. Bialkowski, J. Siegel, C. N. Alfonso, and D. v. d. Linde, Phys. Rev. Lett. **81**, 3679 (1998).
[3] C. Guo, G. Rodriguez, A. Lobad, and A. J. Taylor, Phys. Rev. Lett. **84**, 4493 (2000).
[4] A. Cavalleri, C. Toth, C. W. Siders, J. A. Squier, F. Raksi, P. Forget, and J. C. Kieffer, Phys. Rev. Lett. **87**, 237401 (2001).
[5] T. Ao, Y. Ping, K. Widmann, D. F. Price, E. Lee, H. Tam, P. T. Springer, and A. Ng, Phys. Rev. Lett. **96**, 055001 (2006).
[6] K. Sokolowski-Tinten, J. Bialkowski, and D. v. d. Linde, Phys. Rev. B **51**, 14186 (1995).
[7] I. L. Shumay and U. Hofer, Phys. Rev. B **53**, 15878 (1996).
[8] C. W. Siders, A. Cavalleri, K. Sokolowski-Tinten, C. Toth, T.

Guo, M. Kammler, M. H. v. Hoegen, K. R. Wilson, D. v. d. Linde, and C. P. J. Barty, Science **286**, 1340 (1999).
[9] A. Rousse, C. Rischel, S. Fourmaux, I. Uschmann, S. Sebban, G. Grillon, P. Balcou, E. Foster, J. P. Geindre, P. Audebert, J. C. Gauthier, and D. Hulin, Nature (London) **410**, 65 (2001).
[10] A. M. Lindenberg, J. Larsson, K. Sokolowski-Tinten, K. J. Gaffney, C. Blome, O. Synnergren, J. Sheppard, C. Caleman, A. G. MacPhee, D. Weinstein, D. P. Lowney, T. K. Allison, T. Matthews, R. W. Falcone, A. L. Cavalieri, D. M. Fritz, S. H. Lee, P. H. Bucksbaum, D. A. Reis, J. Rudati, P. H. Fuoss, C. C. Kao, D. P. Siddons, R. Pahl, J. Als-Nielsen, S. Duesterer, R. Ischebeck, H. Schlarb, H. Schulte-Schrepping, T. Tschentscher, J. Schneider, D. v. d. Linde, O. Hignette, F. Sette, H. N. Chapman, R. W. Lee, T. N. Hansen, S. Techert, J. S. Wark, M. Bergh, G. Huldt, D. v. d. Spoel, N. Timneanu, J. Hajdu, R. A. Akre, E. Bong, P. Krejcik, J. Arthur, S. Brennan, K. Luening, and J. B. Hastings, Science **308**, 392 (2005).
[11] E. D. Palik, *Handbook of Optical Constants of Solids* (Academic, New York, 1985).
[12] J. C. Miller, Philos. Mag. **20**, 1115 (1969).
[13] S. Krishnan and P. C. Nordine, Phys. Rev. B **47**, 11780 (1993).
[14] M. A. Havstad, W. McLean II, and S. A. Self, Rev. Sci. Instrum. **64**, 1971 (1993).
[15] L. A. Akashev and V. I. Kononenko, High Temp. **39**, 384 (2001).
[16] L. X. Benedict, J. E. Klepeis, and F. H. Streitz, Phys. Rev. B **71**, 064103 (2005).
[17] H. Ehrenreich, H. R. Philipp, and B. Segall, Phys. Rev. **132**, 1918 (1963).
[18] B. J. Siwick, J. R. Dwyer, R. E. Jordan, and R. J. D. Miller, Science **302**, 1382 (2003).
[19] C. A. D. Roeser, A. M.-T. Kim, P. Callan, L. Huang, E. N. Glezer, Y. Siegal, and E. Mazur, Rev. Sci. Instrum. **74**, 3413 (2003).
[20] S. Backus, J. Peatross, C. P. Huang, M. M. Murnane, and H. C. Kapteyn, Opt. Lett. **20**, 2000 (1995).
[21] C. A. D. Roeser, M. Kandyla, A. Mendioroz, and E. Mazur, Phys. Rev. B **70**, 212302 (2004).
[22] S. A. Kovalenko, A. L. Dobryakov, J. Ruthmann, and N. P. Ernsting, Phys. Rev. A **59**, 2369 (1999).
[23] D. F. Price, R. M. More, R. S. Walling, G. Guethlein, R. L. Shepherd, R. E. Stewart, and W. E. White, Phys. Rev. Lett. **75**, 252 (1995).
[24] J. Hohlfeld, S.-S. Wellershoff, J. Gudde, U. Conrad, V. Jahnke, and E. Matthias, Chem. Phys. **251**, 237 (2000).
[25] P. M. Fauchet, IEEE J. Quantum Electron. **25**, 1072 (1989).
[26] D. v. d. Linde, K. Sokolowski-Tinten, and J. Bialkowski, Appl. Surf. Sci. **109-110**, 1 (1997).
[27] K. Sokolowski-Tinten, J. Bialkowski, A. Cavalleri, D. v. d. Linde, A. Oparin, J. Meyer-ter-Vehn, and S. I. Anisimov, Phys. Rev. Lett. **81**, 224 (1998).
[28] D. v. d. Linde and K. Sokolowski-Tinten, Appl. Surf. Sci. **154-155**, 1 (2000).
[29] B. Huttner, J. Phys.: Condens. Matter **6**, 2459 (1993).
[30] J. D. Jackson, *Classical Electrodynamics*, 3rd ed. (Wiley, New York, 1999).
[31] X. Y. Wang and M. C. Downer, Opt. Lett. **17**, 1450 (1992).
[32] B. Rethfeld, K. Sokolowski-Tinten, and D. v. d. Linde, Phys. Rev. B **65**, 092103 (2002).
[33] L. Huang, P. Callan, E. N. Glezer, and E. Mazur, Phys. Rev. Lett. **80**, 185 (1998).
[34] A. M.-T. Kim, C. A. D. Roeser, and E. Mazur, Phys. Rev. B **68**, 012301 (2003).
[35] P. Borri, F. Romstad, W. Langbein, A. E. Kelly, J. Mork, and J. M. Hvam, Opt. Express **7**, 107 (2000).
[36] Z. Vardeny and J. Tauc, Phys. Rev. Lett. **46**, 1223 (1981).
[37] C. V. Shank and E. P. Ippen, Appl. Phys. Lett. **26**, 62 (1975).
[38] K. L. Hall, G. Lenz, A. M. Darwish, and E. P. Ippen, Opt. Commun. **111**, 589 (1994).
[39] Z. Vardeny and J. Tauc, Opt. Commun. **39**, 396 (1981).